Soft Matter

Cite this: *Soft Matter*, 2011, **7**, 10032

www.rsc.org/softmatter

PAPER

Biocatalytic self-assembly of 2D peptide-based nanostructures†

Meghan Hughes,[a] Haixia Xu,[b] Pim W. J. M. Frederix,[ad] Andrew M. Smith,[c] Neil T. Hunt,[d] Tell Tuttle,[a] Ian A. Kinloch[b] and Rein V. Ulijn*[a]

Received 27th May 2011, Accepted 16th August 2011
DOI: 10.1039/c1sm05981e

Peptide based 2D nanostructures of micronscale size in both X and Y dimensions are extremely rare because amino acid chirality favours helical structures, and nucleation-growth mechanisms usually favour uni-directional growth. We demonstrate the production of extended two-dimensional (2D) peptide nanostructures *via* the thermolysin catalysed condensation of Fmoc protected hydrophilic amino acid (serine, Fmoc-S) and a hydrophobic amino acid ester (phenylalanine, F-OMe). We propose that lateral self-assembly is enabled by the reversible nature of the system, favouring the thermodynamic product (extended sheets) over kinetically favoured 1 dimensional structures. Fmoc-SF-OMe forms extended arrays of β-sheet structures interlock *via* π-stacking between Fmoc groups. We propose that, due to its alternating hydrophilic/hydrophobic amino acid sequence, amphiphilic sheets presenting either phenyl or hydroxyl functionality are formed that assemble pair-wise, thereby shielding hydrophobic groups from the aqueous environment. Formation of these structures was supported by fluorescence emission spectroscopy, FTIR and XRD analysis and molecular mechanics minimization. At enhanced enzyme concentrations, hierarchical self-assembly was observed giving rise to spherulitic structures, with the number of spherulites dictated by enzyme concentration.

Introduction

There is a significant interest in the production of functional materials by exploiting supramolecular chemistry.[1,2] Peptides are of particular interest as building blocks - they have a rich chemical diversity and an inherent ability to effectively interface with biological systems.[3] Peptide based nanostructures usually take the shape of zero- or one-dimensional structures, such as micelles, tubes,[4–6] fibers,[7–9] or (twisted) ribbons.[10] Chiral uni-directional structures are often favoured due to (i) the inherent chirality[11] in peptide building blocks and (ii) the nucleation and growth mechanisms[12] which generally involves formation of nuclei that have a preference to extend uni-directionally. Flat, sheet-like structures based on alternating hydrophobic/hydrophilic polypeptides have already been proposed in the mid-70s[13] and oligopeptides composed of interwoven fibrous networks[14] as well as hybrid polysaccharide/peptide amphiphile membranes[15] have been demonstrated. These systems are 2D at the microscopic and macroscopic length scales but are ultimately composed of 1D fibrillar nanostructures. Peptoids, which are non-chiral polymers with peptide like side chains, were recently shown to form 2D structures.[16] Flat structures with limited lateral directions (belts) were recently described by Cui *et al.*[17] and Shao *et al.*[18] Both systems were based on peptide amphiphiles with alternating hydrophobic and hydrophilic amino acid residues. These sequences are well known to have a predisposition to form β-sheet like structures for oligo-peptides[3,10,14] with a hydrophobic and hydrophilic face, that have a tendency to dimerise, thereby hiding the hydrophobic faces from water. These further assemble to produce tapes and fibres, as discussed above.

Although molecular self-assembly proposes that supramolecular material properties can be fully encoded into molecular building blocks, it is increasingly apparent that the self-assembly pathway largely dictates the final structure.[19] In the biological world, self-assembly processes are commonly coupled to catalysis which enables tight control over the self-assembly pathway. The combination of (bio-) catalysis and molecular self-assembly provides a relatively new concept in laboratory based supramolecular chemistry. The approach consists of converting non-assembling precursors into self-assembly building blocks, usually by enzymatic removal of a charged or steric group that prevents self-assembly,[19–22] or by condensation (reversed hydrolysis) of amino acid derivatives to

[a]*WestCHEM, Department of Pure & Applied Chemistry, University of Strathclyde, Glasgow, UK. E-mail: rein.ulijn@strath.ac.uk*
[b]*School of Materials, University of Manchester, Manchester, UK*
[c]*Lehrstuhl Biomaterialien, University of Bayreuth, Germany*
[d]*SUPA, Department of Physics, University of Strathclyde, Glasgow, UK*

† Electronic Supplementary Information (ESI) available: concentration yield correlations, optical images of precipitates, supporting TEM and SEM images, computer models, chemical synthesis of Fmoc-SF-OMe and characterisation, further WAXS data. See DOI: 10.1039/c1sm05981e/

produce self-assembling peptide amphiphiles.[23] Additionally, the reversibility of the reaction will allow for the formation of the most thermodynamically stable nanostructures.[23]

The self-assembly strategy is based on aromatic peptide amphiphiles, *i.e.* short (generally less than five amino acids) peptides appended with aromatic groups.[6,26–31] These are thought to self-assemble *via* a combination of hydrogen bonding between peptide groups and π-stacking/hydrophobic interactions between aromatic groups. Despite their relative simplicity, the assembly rules are not fully understood with a few exceptions which are composed of aromatic ligands such as N-fluorenyl-9-methoxycarbonyl (Fmoc) or naphthalene derivatives linked to hydrophobic peptides such as FF,[6] LLL,[32] AV[30] giving rise to chiral, 1D nanostructures.

The peptide sequence used here involves a combination of an Fmoc-protected hydrophilic (serine, S) and the methyl ester of a hydrophobic (phenylalanine, F) residue. This combination was found to give rise to stable self-assembling structures. It was previously discovered by using a dynamic combinatorial library[1,33,34] of precursor components, based on Fmoc-amino acids (serine, S and threonine, T) and a range of amino acid methyl esters all present simultaneously in a mixture containing a non-specific protease which was able to catalyse condensation of these residues and with the self-assembly thermodynamics driving the condensation reactions. It was found that Fmoc-SF-OMe was produced preferentially,[35] which indicates it has a strong tendency for molecular self-assembly.

Experimental

Fmoc-S (Bachem, UK) and F-OMe (Sigma-Aldrich, UK) were weighed as a 20 : 80 mM ratio in a glass vial. The powder mixture was dissolved in 2 mL of 0.1 M pH 8 potassium phosphate buffer with the addition of the 1mg ml^{-1} lyophilised *thermolysin* powder (*bacillus Thermoproteolyticus rokko* from Sigma-Aldrich, UK) unless otherwise stated. The solution was vortexed and sonicated to ensure dissolution. Samples were incubated at room temperature.

HPLC

A Dionex P680 system operating with a Macherey-Nagel 250 Å, 4.6 × 250 mm, C18 column was used for reversed phase HPLC. 10 μL of sample was injected. The mobile phase was comprised of water and acetonitrile ramped from 20–80% over 35 min at a flow rate of 1 mL min^{-1}. Detection of the peptide amphiphiles was carried out using a UVD170U UV-Vis detector at a 300 nm wavelength.

Fluorescence

Fluorescence emission spectra were measured on a Jasco FP-6500 spectrofluorometer with fluorescence measured orthogonally to the excitation light with a scanning speed of 200 nm min^{-1}. Excitation light at 280 nm and emission data range between 300 nm and 600 nm. The emission spectra were measured with a bandwith of 3 nm with a medium response and a 1 nm data pitch. Spectra were normalised to maximum intensity.

FTIR

FTIR spectra were acquired in a Bruker Vertex spectrometer with a spectral resolution of 2 cm^{-1}. The spectra were obtained by averaging 64 interferograms for each sample. Measurements were performed in a standard IR cuvette (Harrick Scientific), in which the sample was contained between two CaF_2 windows (thickness, 2 μm) separated by a 25-μm PTFE spacer. All sample manipulations were performed in a glove box to minimize interference from atmospheric water vapour; D_2O was used as the solvent for all the IR measurements.

WAXS

WAXS analysis were performed using a Philips X'Pert diffractometer with a wavelength of 1.5406 Å. Fmoc-SF-OMe gel and buffer solution were spread on two separate silica substrates as film and allowed to air dry prior to data collection.

TEM

Carbon-coated copper grids (200 mesh) were glow discharged in air for 30 s. A 10 μL volume of gel was transferred onto the support film and blotted down using filter paper. 20 μl of negative stain (1% aqueous methylamine vanadate obtained from Nanovan; Nanoprobes) was applied and the mixture blotted again using filter paper to remove excess. The dried specimens were then imaged using a LEO 912 energy filtering transmission electron microscope operating at 120kV fitted with 14bit/2 K Proscan CCD camera.

CryoTEM

Gel samples were blotted onto a thin film grid of 100–200 nm. The grid was then plunged into liquid ethane (temperatures below −170 °C) and transferred to a GATAN 626 cryoholder and imaged using a JEOL 2100 transmission electron microscope fitted with a GATAN 4 K Ultrascan camera. The cryoTEM analysis was carried out at Unilever, Bedford.

Optical microscopy

10 μL of sample was transferred onto a glass slide and covered with a cover slip. The samples were then examined using a Zeiss Axio Imager A1 optical microscope equipped with polarising lenses at 0° using a bright lens and transmitted light. Homogeneity was ensured by repeating in triplicate.

Synthesis of Fmoc-SF-Ome

Fmoc-S (1 g, 2.8 mM), F-OMe (0.72g, 3.4 mM) and HBTU (1.26g, 3.4 mM) were dissolved in 10 mL of DMF. 1.041 mL (5.6 mM) of DIPEA was added and solution stirred for 24 h. The solvent was removed by evaporation *in vacuo*. The resulting solid was dissolved in ethyl acetate, washed in duplicate with equal volumes of 1M sodium bicarbonate, brine and 1 M HCl. The organic layer dried using sodium sulphate and filtered. Solvent removed by evaporation *in vacuo*. The white solid then purified over a silica column using 2.5%–7.5% methanol in chloroform. Aliquots evaporated at room temperature and pressure and white solid combined (21% yield, 98% purity).

Computer modelling

All structures were constructed in ArgusLab[36] and subsequently energy-minimized in vacuum using the conjugate gradient method as implemented in NAMD.[37] The minimization procedure was carried out for 10,000 steps, at which point the fluctuations in the energy were $<10^{-4}$ kcal mol^{-1} and the structure was considered to be converged. The CHARMM c36a3 force field[38] was used to minimize the structure. VMD[39] was used to visualize the results.

Results and discussion

Condensation of Fmoc-S, **1**, and F-OMe, **2** in a 1 : 4 ratio by thermolysin from *Bacillus thermoproteolyticus rokko* resulted in formation of Fmoc-SF-OMe, **3**, (Fig. 1(a)) at a constant conversion of 98% after 24 h with an initial reactant concentration of 20/80 mM.[35] The system exhibits typical equilibrium behaviour, with higher yields of **3** formed at corresponding increased concentrations of starting materials (see ESI,† Fig. S1). Rather than forming translucent hydrogels typically observed for aromatic peptide amphiphiles,[6,26–32] the self-assembly results in a weak opaque suspension which remains stable over a number of weeks (see Fig. 1(b)). It should be noted that the chemically synthesised compound **3**, in a pure state or as a 1 : 3 mixture of compounds **3** and **2**, forms amorphous precipitates in buffer with no evidence of formation of ordered nanostructures (see ESI,† Fig. S2). Initial investigation of the self-assembled structure was carried out using TEM and cryoTEM (see Fig. 1(c)–(d)and additional fields of view supplied in ESI,† Fig. S3). This revealed sheet-like structures of many microns in both X and Y dimensions, in addition to twisted nano-ribbons.

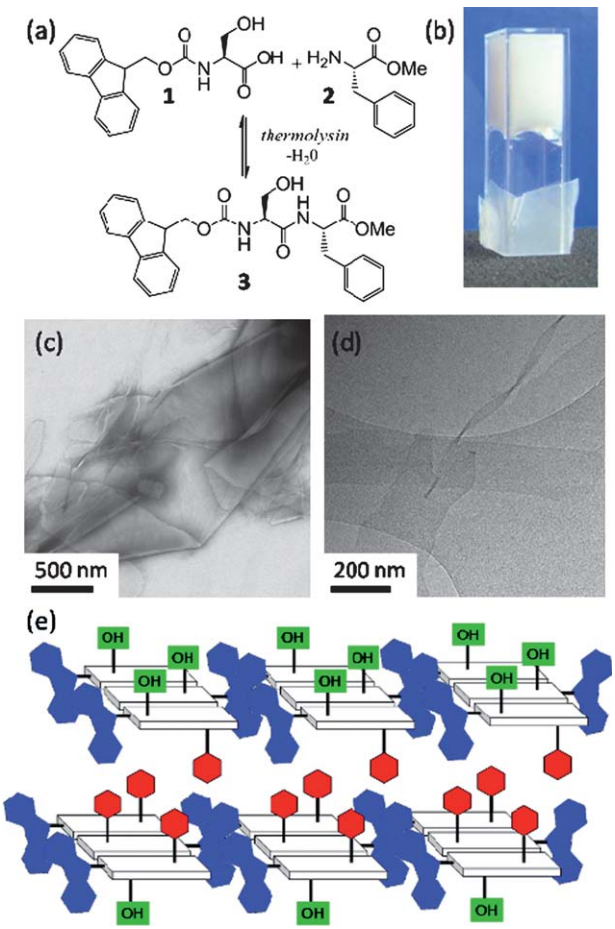

Fig. 1 (a) reaction scheme of Fmoc-S, **1**, coupled with F-OMe, **2**, to form Fmoc-SF-OMe, **3**, *via* condensation using protease enzyme *thermolysin*. (b) **3** self-assembles to form nano-sheets within a self-supporting opaque suspension. (c) and (d) TEM and Cryo-TEM images of nano-sheets of **3** obtained after 24 h. (e) The schematic representation of the molecular assembly of **3** to form bilayer nano-sheets.

Fluorescence emission spectroscopy was used to monitor changes in fluorenyl environment as the reaction proceeded (see Fig. 2(a)). It should be noted that a substantial reduction in signal intensity was observed over time, this is, at least in part, due to the sample becoming increasingly opaque. The spectra were normalised to allow a more accurate determination of peak formation and shifting; whilst original intensity changes of each peak of interest are shown in Fig. 2(b). It is evident that a number of structural changes occur. The starting mixture shows two predominant features emitting at approximately 320 and 330 nm, representing monomeric and aggregated forms of Fmoc-S precursors. Within 10 min a red shift accompanied by an increase in intensity indicates a supramolecular transition producing a more intensely emitting fluorenyl species. The formation of a red-shifted peak at 365 nm accompanied by system quenching (Fig. 2(b)) could be associated with formation of extended aggregates through π- stacked systems as previously observed, *e.g.* for Fmoc-LLL[32] and Fmoc-FF.[6a,d] However, it should be noted that the red-shift is much less pronounced for the system under study, suggesting that fluorenyl face to face π-stacking may not be optimal in these systems. After 24 h, the free fluorenyl peak has nearly disappeared, suggesting that few Fmoc-S or Fmoc-SF-OMe species are in the un-assembled state, which is consistent with the condensation yield observed.

The hydrogen bonding interactions of peptide moieties of **3** were then monitored using FTIR spectroscopy focusing on carbonyl stretching in the amide I region. Fig. 2(c) illustrates the time-dependent correlation peaks at 1640 cm^{-1}, 1680 cm^{-1} and 1650 cm^{-1} peak intensities. As they all appear at the same point over the reaction coordinate it can be assumed that they represent the molecular organisation of nanostructural sheets. The pair of peaks at 1640 cm^{-1} and 1680 cm^{-1} are characteristic of the formation of a β-sheet arrangement of the peptide moieties (see Fig. 2(d)).[6,32,40] This structure becomes evident from 5 h and also remains in this arrangement over 72 h. It is noticeable that the peaks gradually shift to lower frequencies during this time, consistent with hydrogen bonding strength increasing. This is accompanied by the occurrence of a peak due to the carbonyl stretch associated with the methyl ester moiety at 1728 cm^{-1} in addition to the peak at 1745 cm^{-1} attributable to the carbonyl of free F-OMe. However, a prominent peak at 1650 cm^{-1}, indicative of random order of peptides[40] is also present, which indicates that although the structure is organised as an extended anti-parallel β-sheet arrangement, there is also a disordered component. In contrast to the similar dynamics of the FTIR peaks located at 1640 and 1680 cm^{-1} (beta sheet) and 1650 cm^{-1} (pseudo random coil), it is interesting to note the

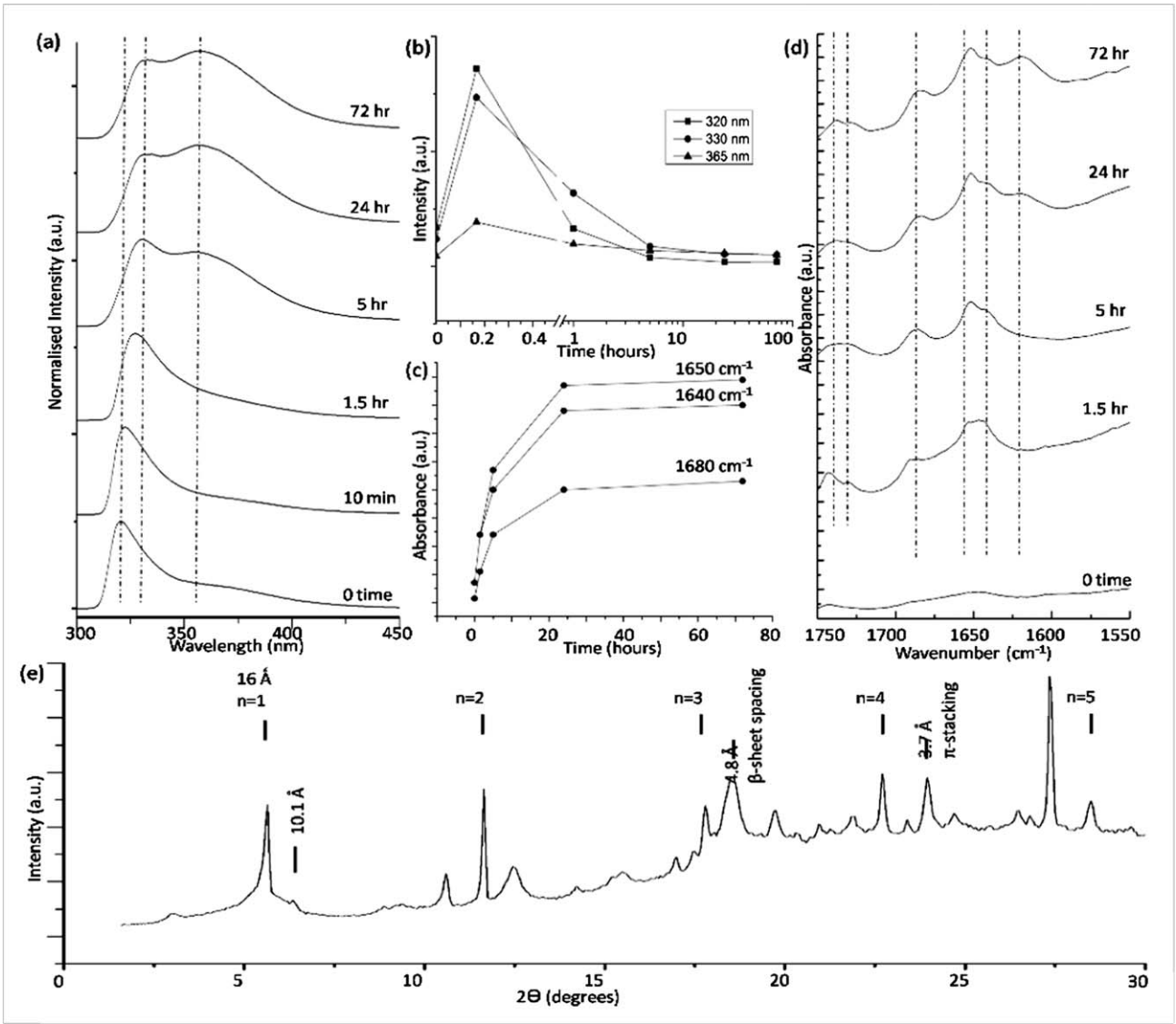

Fig. 2 (a) Fluorescence emission spectra monitored over 72 h. (b) Relative intensity of 320 nm, 330 nm and 365 nm peaks within fluorescence spectra monitored with time (intensity normalised). (c) Relative intensity of 1640 cm^{-1}, 1680 cm^{-1} and 1650 cm^{-1} bands within FTIR spectra monitored with time. (d) Amide I region of FTIR absorbance spectra monitored over 72 h, representing carbonyl stretching mode of amino acid residues. (e) WAXS data of dried sample at 24 h.

appearance of the peak at 1620 cm^{-1}, which occurs only after 24 h. The assignment of this peak is currently unclear but the timescales are consistent with higher order structure formation of spherulites as discussed below.‡

In order to confirm the proposed structure, WAXS diffraction patterns were obtained (see Fig. 2(e)). A prominent peak with 5 higher order reflections indicates a repeating pattern of 16 Å which we have correlated to the repeating unit along the peptide backbone, and additional peaks corresponding to 4.8 Å and 3.7 Å which relate to β- sheet spacing and π-stack spacing respectively.[32] Typically, this type of π-interlocked β-sheet (π-β) molecular association results in fibrillar network structures,[6a,32] but has also been observed to produce belts when Fmoc-dipeptides with hydrophilic and (modified) hydrophobic residues were used.[18] We propose a model that is consistent with these reflections obtained for the WAXS data and the observed planar sheets (see Fig. 3). The Fmoc-groups form stacked pairs rather than a continuous π-stack proposed for Fmoc-FF.[6a,d] In that system, the C-terminal phenyl group intercalated between the Fmoc groups to create a continuous π- stack. In the case of Fmoc-SF-OMe the methyl ester prevents the molecules assuming this configuration, which would also explain the absence of a 450 nm peak observed in fluorescence by Smith *et al.*[6a] and Xu *et al.*[32] The phenyl moieties of phenylalanine residues can interact with those from a neighbouring array to form the π-β bilayer as illustrated in Fig. 3. This molecular association also explains the formation

‡ The assignment of this peak is not clear though it is consistent with intermolecular beta sheet formation observed in proteins and may indicate a secondary interaction of beta sheet structures as the time scales are consistent with higher order structure formation of spherulites.

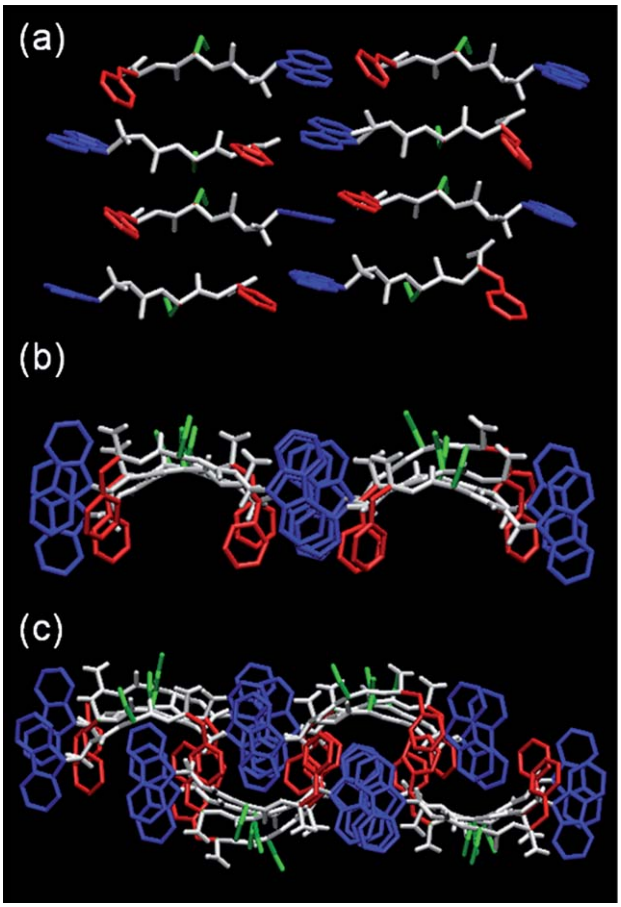

Fig. 3 Molecular association models. (a) 8-mer anti-parallel β-sheet arrangement. (b) 8-mer side view. (c) 16-mer side view of two separate 8-mers where their hydrophobic residues interact to from a bilayer.

of extended 2D structures rather than 1D fibers or tubes, since next to the π-stacking of fluorenyl groups and anti- parallel β-sheets there is a driving force that extends the structure in a biaxial direction, yet keeping its linearity. Overall, this assembly results in the hydrophobic phenylalanines being completely buried within the bilayer, while the hydrophilic serine residues are orientated outwards and can hydrogen bond to the aqueous environment or with serine residues of a neighbouring self-assembled bilayer system to produce multi-bilayers, similar to Shao *et al.*[18] and to well-documented bilayered tapes in larger β-sheet self-assembling peptides.[10,41] From the structure in Fig. 3 a 64-mer was built of 8 × 4 × 2 molecules (see ESI,† Fig. S4). The proposed structure proved to be stable under minimization using molecular mechanics, and exhibits repeating units with average distances of 16.2 Å (Fmoc-column to Fmoc-column), 4.9 Å (peptide backbone to backbone), and 3.7 Å (Fmoc- to Fmoc- within the π-stacked columns), which are in excellent agreement with the reflections observed in WAXS. Additionally, 10.1 Å can be observed for Fmoc-pair to Fmoc-pair in the stacking direction, which also corresponds to a peak on the WAXS data (see Fig. 2(d)). The proposed model is also consistent with the other spectroscopic results such as the formation of stable β-sheets observed from FTIR. The minimized model also shows that the methyl ester may form an intramolecular hydrogen bond with the serine hydroxyl group, which may explain the observed shift in the methyl ester peak (see Fig. 2(d)).

In previous systems,[17,18] growth has always been predominantly along one axis unless the chirality of the peptides has been removed, and the nanostructure is comprised solely of non-natural peptides forming crystalline sheets.[16] In certain cases, for example in β-hairpin assemble, lateral growth is unfavoured because all peptides assembling in register, in which case the width is dictated by peptide length.[8] In cases where lateral association through formation of 'sticky ends' is possible, it remains unknown as to what causes such growth restrictions.[17,18] It is most likely related to the size of initial nuclei which have a preference to grow uni-directionally, *i.e.* a kinetic effect. A key difference in the system described here, is that the building blocks themselves can be reversibly formed and hydrolysed, giving rise to a system which will be less prone to kinetic locking.

TEM images suggest a mechanism for sheet formation, where twisted tapes are predominantly observed at the early stages (see ESI,† Fig. S5). 24 h after the reaction has been initiated, branching of the twisted nanoribbons and nucleation of ribbons from the edge of sheets is observed. The images suggest a progression through several phases before reaching the final sheet structures, which we believe to be related to constant enzymatic structure correction at the edges of existing structures.

During the latter stages of self-assembly (24–72 h), a remarkable further hierarchical self-assembly was observed which is tunable by enzyme concentration. SEM analysis reveals that macroscopic spherulitic structures are formed of several hundred microns in diameter (see Fig. 4). These spherulites are surrounded by non-spherulitic areas of material being constructed of layered lamellar structures, thought to represent multilayers of the 2D sheets discussed, which could feasibly interact *via* hydrogen bonding of the exposed hydroxyl groups of the serine residues. Higher magnification SEM images of the spherulitic structures shows that these structures are composed of sheets, with no obvious nucleation points at their centres. Peptide based spherulitic structures have been obtained previously by solvent induced phase transitions[42] or by hierarchical assembly from aromatic peptide amphiphiles.[43]

It has previously been demonstrated that self-assembly is favoured in the direct vicinity of enzymes[23–25] and therefore it is tempting to propose enzymatic control of spherulite formation. To investigate a possible link between enzyme concentration and spherulite formation, a range of enzyme concentrations (0.1, 1, 10 mg mL^{-1}) were analysed using polarising optical microscopy. The spherulites display birefringence when viewed under cross polarisers (see Fig. 5). Each of the samples appear as opaque suspensions at 24 h. However, the rate at which each becomes self-supporting varies; 0.1 mg mL^{-1} *thermolysin* after approximately 24 h, 1 mg mL^{-1} within a matter of hours, and 10 mg mL^{-1} after only a few minutes of the reaction being initiated; which is to be expected. At a low enzyme concentration of 0.1 mg mL^{-1}, no spherulitic structures form. This has been further confirmed by the formation of solely the layered lamellar structures visible using SEM (see ESI,† Fig. S6). Additionally, the use of a higher enzyme concentration (10 mg mL^{-1}) displayed a dramatic increase in the number of these spherulitic structures are formed (see Fig. 5). This signifies that the enzyme plays a key

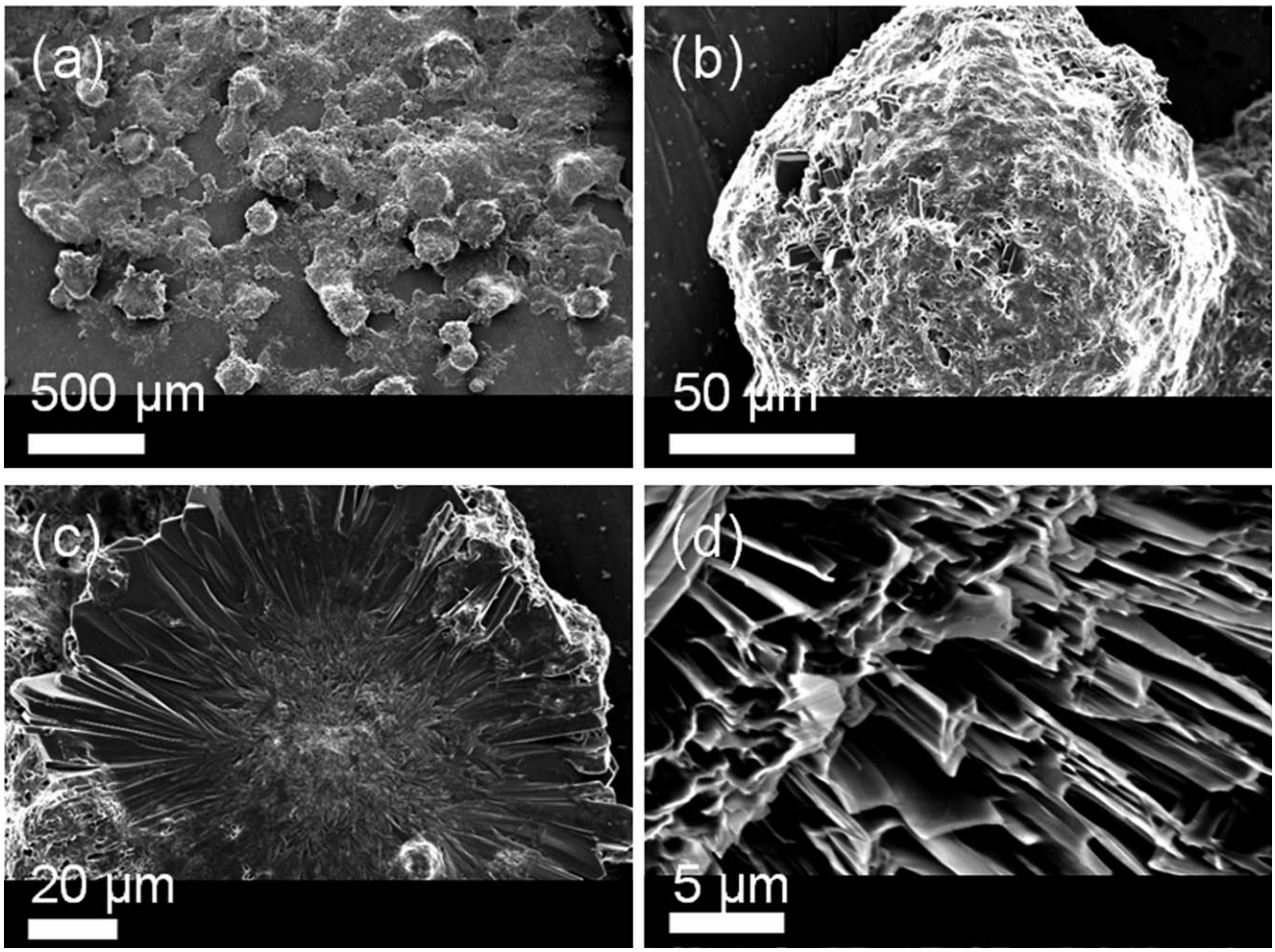

Fig. 4 SEM imaging of self-assembled Fmoc-SF-OMe. (a) Spherical structures and 'halved' spherical structures can been seen to lie on a layer of the nano-sheet material. (b) Spherical structures encased in nano-sheet material. (c,d) Spherical structures have crystalline spherulitic centres with no obvious nucleation point and are surrounded by a layer of sheets. (d) Lamellar structure of non-spherulitic areas.

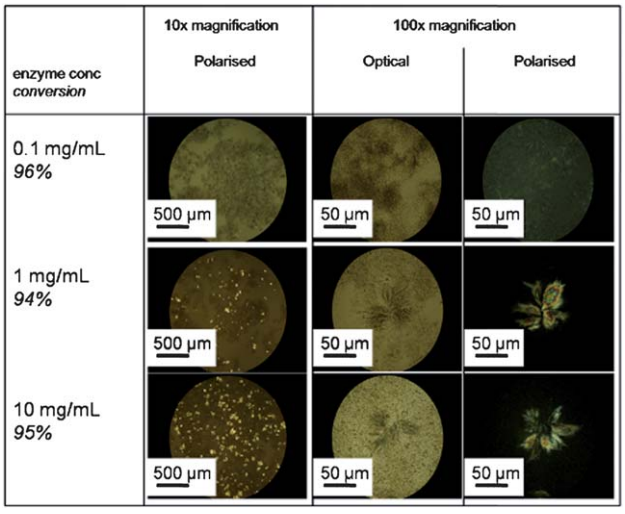

Fig. 5 Optical and polarised images of macrostructure. Birefringence or crystalline structures is observed when viewed under cross-polarisers. A relationship between enzyme concentration and number of spherulitic structures is observed.

role in nucleation process to form these spherulites, however it does not affect the ultimate size of the crystals (diameter of just over 100 μM).

Conclusions

In summary, we have demonstrated a route towards the production of two-dimensional nanostructures by enzymatic condensation of chiral amino acid derivatives. We propose that lateral self-assembly is enabled by the reversible nature of the system, favouring the thermodynamic product (extended sheets) over kinetically favoured 1 dimensional structures. The combination of hydrophilic and hydrophobic amino acids, which are interlocked *via* π-stacking interactions of Fmoc groups, produce amphiphilic bilayers, with the hydrophobic faces hidden from water and further stabilised *via* π-stacking of phenyl rings. The production of nano-sheets with well-defined chemical composition is of interest in production of surfaces with precisely presented bioactivity, and may also be used in templating,[44,45] and by combination with biocatalysis, dynamic template structures may be feasible.[46,47] The remarkable structural,[3–6] biological,[7–9] and electronic[18,32] properties of peptide based nanostructures, combined with the low cost of materials based on dipeptides or

amino acid derivatives, suggests future applications in material science, biomedicine and nanotechnology.

References

1 J. M. Lehn, *Supramolecular Chemistry - Concepts and Perspectives*, VCH, Weinheim, 1995.
2 G. M. Whitesides and B. Grzybowski, *Science*, 2002, **295**, 2418.
3 (*a*) X. B. Zhao, F. Pan, H. Xu, M. Yaseen, H. H. Shan, C. A. E. Hauser, S. G. Zhang and J. R. Lu, *Chem. Soc. Rev.*, 2010, **39**, 3480; (*b*) I. W. Hamley, *Soft Matter*, 2011, **7**, 4122; (*c*) M. Zelzer and R. V. Ulijn, *Chem. Soc. Rev.*, 2010, **39**, 3351.
4 M. R. Ghadiri, J. R. Granja, R. A. Milligan, D. E. McRee and N. Khazanovich, *Nature*, 1993, **366**, 324.
5 M. Reches and E. Gazit, *Science*, 2003, **300**, 625.
6 (*a*) A. M. Smith, R. J. Williams, C. Tang, P. Coppo, R. F. Collins, M. L. Turner, A. Saiani and R. V. Ulijn, *Adv. Mater.*, 2008, **20**, 37; (*b*) V. Jayawarna, M. Ali, T. A. Jowitt, A. F. Miller, A. Saiani, J. E. Gough and R. V. Ulijn, *Adv. Mater.*, 2006, **18**, 611–614; (*c*) A. Mahler, M. Reches, M. Rechter, S. Cohen and E. Gazit, *Adv. Mater.*, 2006, **18**, 1365; (*d*) C. Tang, A. M. Smith, R. F. Collins, R. V. Ulijn and A. Saiani, *Langmuir*, 2009, **25**, 9447.
7 G. A. Silva, C. Czeisler, K. L. Niece, E. Beniash, D. A. Harrington, J. A. Kessler and S. I. Stupp, *Science*, 2004, **303**, 1352.
8 L. Haines-Butterick, K. Rajagopal, M. Branco, D. Salick, R. Rughani, M. Pilarz, M. S. Lamm, D. J. Pochan and J. P. Schneider, *Proc. Natl. Acad. Sci. U. S. A.*, 2007, **104**, 7791.
9 E. F. Banwell, E. S. Abelardo, D. J. Adams, M. A. Birchall, A. Corrigan, A. M. Donald, M. Kirkland, L. C. Serpell, M. F. Butler and D. N. Woolfson, *Nat. Mater.*, 2009, **8**, 596.
10 A. Aggeli, M. Bell, N. Boden, J. N. Keen, P. F. Knowles, T. C. B. McLeish, M. Pitkeathly and S. E. Radford, *Nature*, 1997, **386**, 259.
11 P. Jonkheijm, P. van der Schoot, A. P. H. J. Schenning and E. W. Meijer, *Science*, 2006, **313**, 80.
12 J. Cornelissen, A. E. Rowan, R. J. M. Nolte and N. Sommerdijk, *Chem. Rev.*, 2001, **101**, 4039.
13 A. Brack and L. E. Orgel, *Nature*, 1975, **256**, 383.
14 S. G. Zhang, T. Holmes, C. Lockshin and A. Rich, *Proc. Natl. Acad. Sci. U. S. A.*, 1993, **90**, 3334.
15 R. M. Capito, H. S. Azevedo, Y. S. Velichko, A. Mata and S. I. Stupp, *Science*, 2008, **319**, 1812.
16 K. T. Nam, S. A. Shelby, P. H. Choi, A. B. Marciel, R. Chen, L. Tan, T. K. Chu, R. A. Mesch, B. C. Lee, M. D. Connolly, C. Kisielowski and R. N. Zuckermann, *Nat. Mater.*, 2010, **9**, 454.
17 H. Cui, T. Muraoka, A. G. Cheetham and S. I. Stupp, *Nano Lett.*, 2009, **9**, 945.
18 H. Shao and J. Parquette, *Chem. Commun.*, 2010, **46**, 4285.
19 A. R. Hirst, S. Roy, M. Arora, A. K. Das, N. Hodson, P. Murray, N. Javid, J. Sefcik, J. Boekhoven, J. H. van Esch, S. Santabarbara, N. T. Hunt and R. V. Ulijn, *Nat. Chem.*, 2010, **2**, 1089–1094.
20 (*a*) Z. M. Yang, H. W. Gu, D. G. Fu, P. Gao, J. K. Lam and B. Xu, *Adv. Mater.*, 2004, **16**, 1440; (*b*) Y. Zhang, H. W. Gu, Z. M. Yang and B. Xu, *J. Am. Chem. Soc.*, 2003, **125**, 13680.
21 S. Winkler, D. Wilson and D. L. Kaplan, *Biochemistry*, 2000, **39**(12), 739.
22 C. Wang, Q. Chen, Z. Wang and X. Zhang, *Angew. Chem., Int. Ed.*, 2010, **49**, 8612.
23 (*a*) S. Toledano, R. J. Williams, V. Jayawarna and R. V. Ulijn, *J. Am. Chem. Soc.*, 2006, **128**, 1070; (*b*) R. J. Williams, A. M. Smith, R. Collins, N. Hodson, A. K. Das and R. V. Ulijn, *Nat. Nanotechnol.*, 2009, **4**, 19.
24 R. de la Rica, K. I. Fabijanic, A. Baldi and H. Matsui, *Angew. Chem. Int. Ed.*, 2010, **49**, 1447.
25 H. Wang, Z. Wang, D. Song, J. Wang, J. Gao, L. Wang, D. Kong and Z. Yang, *Nanotechnology*, 2010, **21**, 155602.
26 R. Vegners, I. Shestakova, I. Kalvinsh, R. M. Ezzell and P. A. Janmey, *J. Pept. Sci.*, 1995, **1**, 371.
27 D. M. Ryan, T. M. Doran, S. B. Anderson and B. L. Nilsson, *Langmuir*, 2011, **27**, 4029.
28 S. Debnath, A. Shome, D. Das and P. K. Das, *J. Phys. Chem. B*, 2010, **114**, 4407.
29 (*a*) L. Chen, K. Morris, A. Laybourn, D. Elias, M. R. Hicks, A. Rodger, L. Serpell and D. J. Adams, *Langmuir*, 2010, **26**, 5232; (*b*) E. K. Johnson, D. J. Adams and P. J. Cameron, *J. Mater. Chem.*, 2011, **21**, 2024.
30 G. Cheng, V. Castelletto, C. M. Moulton, G. E. Newby and I. W. Hamley, *Langmuir*, 2010, **26**, 4990.
31 D. Bardelang, F. Camerel, J. C. Margeson, D. M. Leek, M. Schutz, B. Zaman, K. Yu, D. V. Soldatov, R. Ziessel, C. I. Ratcliffe and J. A. Ripmeester, *J. Am. Chem. Soc.*, 2008, **130**, 3313.
32 H. Xu, A. K. Das, M. Horie, M. S. Shaik, A. M. Smith, Y. Luo, X. Lu, R. Collins, S. Y. Liem, S. Song, P. L. A. Popelier, M. L. Turner, P. Xiao, I. A. Kinloch and R. V. Ulijn, *Nanoscale*, 2010, **2**, 960.
33 N. Sreenivasachary and J. M. Lehn, *Proc. Natl. Acad. Sci. U. S. A.*, 2005, **102**, 5938.
34 S. Otto, R. L. E. Furlan and J. K. M. Sanders, *Science*, 2002, **297**, 590.
35 A. K. Das, A. R. Hirst and R. V. Ulijn, *Faraday Discuss.*, 2009, **143**, 293.
36 M. A. Thompson, 2004, *ArgusLab 4.0.1*, Seattle, WA Planaria Software LLC.
37 J. C. Phillips, R. Braun, W. Wang, J. Gumbart, E. Tajkhorshid, E. Villa, C. Chipot, R. D. Skeel, L. Kale and K. Schulten, *J. Comput. Chem.*, 2005, **26**, 1781.
38 B. R. Brooks, *et al.*, *J. Comput. Chem.*, 2009, **30**, 1545.
39 W. Humphrey, A. Dalke and K. Schulten, *J. Mol. Graphics*, 1996, **14**, 33.
40 A. Barth and C. Zscherp, *Q. Rev. Biophys.*, 2002, **35**, 369.
41 H. Yokoi, T. Kinoshita and S. Zhang, *Proc. Natl. Acad. Sci. U. S. A.*, 2005, **102**, 8414.
42 P. Zhu, X. Yan, Y. Su, Y. Yang and J. Li, *Chem.–Eur. J.*, 2010, **16**, 3176.
43 W. Wang and Y. Chau, *Soft Matter*, 2009, **5**, 4893.
44 N. Sharma, A. Top, K. L. Kiick and D. J. Pochan, *Angew. Chem., Int. Ed.*, 2009, **48**, 7078.
45 M. S. Lamm, N. Sharma, K. Rajagopal, F. L. Beyer, J. P. Schneider and D. J. Pochan, *Adv. Mater.*, 2008, **20**, 447.
46 F. Patolsky, Y. Weizmann and I. Willner, *Nat. Mater.*, 2004, **3**, 692.
47 N. Ostrov and E. Gazit, *Angew. Chem., Int. Ed.*, 2010, **49**, 3018.

